Communications on Applied Nonlinear Analysis
ISSN: 1074-133X
Vol 31 No. 8s (2024)

Two Fluid Interacting and Non-Interacting Scenarios for Kaluza-Klein Dark Energy Cosmological Model in Lyra Geometry

Parimal Gaidhane[1], A. M. Pund[2]

[1](Research Scholar, Department of Mathematics, S. S. E. S. Amravati's Science College, Congress Nagar, Nagpur, India-440012, parimalgaidhane95@gmail.com)

[2](Associate Professor, Department of Mathematics, S. S. E. S. Amravati's Science College, Congress Nagar, Nagpur, India-440012, ashokpund64@rediffmail.com)

Article History:

Received: *10-10-2024*

Revised: *20-11-2024*

Accepted: *29-11-2024*

Abstract:

In this paper, we studied the evaluation of dark energy parameter in the spatial homogeneous and anisotropic five dimensional Kaluza-Klein space time filled with barotropic fluid and dark energy within the frame- work of Lyra geometry. To solve the Einstein field equation by considering the shear scalar (σ) in these models is proportional to expansion scalar (θ). Here we consider two cases; (a) when these fluids are not interacting with each other and, (b) when these fluids interact with each other. We examined the physical and geometric properties and analysed their graphical characteristics. In addition, we investigated several cosmological parameters, look-back time, proper distance, luminosity distance, angular diameter distance and distance modulus.

Keywords: Dark energy, Barotropic fluid, five-dimensional Kaluza-Klein spacetime, Lyra geometry

1. Introduction

Dark energy is a critical factor in understanding cosmological phenomena. Recent astronomical observations [1-4] reveal that the observable universe is currently undergoing accelerated expansion. This acceleration is widely attributed to the influence of dark energy, whose fundamental nature remains one of the central enigmas in modern cosmology. According to estimates from the Wilkinson Microwave Anisotropy Probe (WMAP), the composition of the universe comprises approximately 73% dark energy, 23% dark matter, and 4% ordinary matter. Various cosmological models, such as the cosmological constant [5], quintessence [6], equation of state parameterizations [7-11], and interactive dark energy models [12-18], have been proposed to explore the properties of dark energy and its role in driving the universe's accelerating expansion.

Einstein formulated the field equations of general relativity using the principles of gravitational geometry. Building on these ideas, Weyl [19] proposed a geometric framework integrating gravity and electromagnetism. However, Weyl's theory was ultimately dismissed due to the inability to integrate vector lengths under parallel displacement. In response, Lyra introduced a modification to Riemannian geometry that incorporates gauge functions in manifolds, offering an alternative that diverges from the structure of Weyl geometry. This development spurred further research into scalar-tensor theories and cosmology within the context of Lyra geometry. Sen [20] and Sen and Dunn [21] extended this work, formulating a novel scalar-tensor theory of gravity and deriving an analogue of Einstein's field equations based on Lyra geometry. Halford [22] demonstrated that scalar-tensor theories derived from Lyra geometry yield predictions consistent with those of general relativity. Subsequent studies have focused on cosmological models grounded in Lyra geometry, with contributions from several

researchers. Recent investigations by V. G. Mete et al. [23], P. M. Lambat et al. [24], Y. Aditya et al. [25], J. K. Singh et al. [26], and Bishi et al. [27] have explored diverse aspects of these models, further enriching the understanding of Lyra-based cosmological frameworks.

High-dimensional cosmology is pivotal in understanding the early stages of the universe's evolution immediately following the Big Bang. Over time, the universe condensed into its present four-dimensional form. Prominent researchers such as Witten [28] and Appelquist et al. [29] have extensively studied the implications of higher-dimensional cosmology. In the context of Kaluza-Klein five-dimensional geometry (proposed by Kaluza [30] and Klein [31]), additional spatial dimensions are employed to unify gravity and electromagnetism. This framework introduced the concept of the "cosmological reduction process," where the extra dimensions contract to scales so minute that they become undetectable. The dynamic contraction of extra dimensions was further explored by Chodos and Detweller [32] and Freund and Hawking [33], who demonstrated that these dimensions are rendered imperceptible due to their diminishing scale. Kaluza-Klein cosmological models have been examined extensively within the framework of Lyra geometry. Studies by Pawar et al. [34], Y. Aditya et al. [35], and Mishra et al. [36] have delved into these models in Lyra geometry, while research by V. G. Mete et al. [37], D. Trivedi et al. [38], and M. V. Santhi et al. [39] has focused on incorporating dark energy and barotropic fluid into various cosmological scenarios.

In this study, we explore the estimation of dark energy parameters within a five-dimensional homogeneous and anisotropic Kaluza-Klein spacetime, incorporating a barotropic fluid and dark energy. Section 2 outlines the metric and field equations that form the basis of the analysis. Section 3 focuses on deriving solutions to the field equations and determining relevant physical and geometric parameters. In Section 4, we examine two scenarios involving fluid interactions: interacting and non-interacting fluids. Section 5 is dedicated to the computation of various cosmological parameters, while Section 6 presents the conclusions drawn from the study.

2. Metric and Field Equation

We consider the spatially homogeneous and anisotropic five-dimensional Kaluza-Klein space-time given by,

$$ds^2 = dt^2 - A^2(dx^2 + dy^2 + dz^2) - B^2 d\psi^2 \tag{1}$$

where, A and B are functions of cosmic time t only and the fifth coordinate ψ is assumed to be space-like co-ordinate

Einstein's field equation is given by,

$$R_i^j - \frac{1}{2}Rg_i^j + \frac{3}{2}\phi_i\phi^j - \frac{3}{4}g_i^j\phi_a\phi^a = -8\pi T_i^j \tag{2}$$

where ϕ_i a displacement field vector is defined $\phi_i = (0,0,0,0,\beta(t))$, and other symbols have their usual meaning, as in Riemannian geometry.

The energy momentum tensor for two fluid is given by,

$$T_i^j = T_i^j(B) + T_i^j(D) \tag{3}$$

where $T_i^j(B)$ and $T_i^j(D)$ represents energy momentum tensor for Barotropic fluid and Dark energy respectively.

Also,

$$T_i^j(B) = (\rho_B + p_B)u_i u^j - p_B g_i^j \tag{4}$$

$$T_i^j(D) = (\rho_D + p_D)u_i u^j - p_D g_i^j \tag{5}$$

Where ρ_B and ρ_D represents the energy density of Barotropic fluid and Dark energy, respectively. Also p_B and p_D represents the pressure of Barotropic fluid and Dark energy, respectively.

The equation of state parameter (ω), which is considered an important quantity for describing the dynamics of the universe, is the ratio of the pressure (p) to the energy density (ρ) and is given by

$$\omega_B = \frac{p_B}{\rho_B} \tag{6}$$

$$\omega_D = \frac{p_D}{\rho_D} \tag{7}$$

The Einstein field equation (2) and (3) for the metric (1), it follows that

$$2\frac{\ddot{A}}{A} + \frac{\ddot{B}}{B} + \frac{\dot{A}^2}{A^2} + 2\frac{\dot{A}\dot{B}}{AB} = -8\pi(p_B + p_D) - \frac{3}{4}\beta^2 \tag{8}$$

$$3\frac{\ddot{A}}{A} + 3\frac{\dot{A}^2}{A^2} = -8\pi(p_B + p_D) - \frac{3}{4}\beta^2 \tag{9}$$

$$3\frac{\dot{A}^2}{A^2} + 3\frac{\dot{A}\dot{B}}{AB} = -8\pi(\rho_B + \rho_D) + \frac{3}{4}\beta^2 \tag{10}$$

The energy conservation equation $T^{j}_{i\,;j} = 0$ gives,

$$(\dot{\rho_B} + \dot{\rho_D}) + (\rho_B + \rho_D + p_B + p_D)\left(3\frac{\dot{A}}{A} + \frac{\dot{B}}{B}\right) = 0 \tag{11}$$

And

$$\left(R^j_i - \frac{1}{2}Rg^j_i\right)_{;j} + \frac{3}{2}(\phi_i\phi^j)_{;j} - \frac{3}{4}\left(\phi_a\phi^a g^j_i\right)_{;j} = 0 \tag{12}$$

Equation (10) gives,

$$\frac{3}{2}\beta\dot{\beta} + \frac{3}{2}\beta^2\left(3\frac{\dot{A}}{A} + \frac{\dot{B}}{B}\right) = 0 \tag{13}$$

3. Solution of the field equations:

Equations (6)-(9) and (11) are five equations with seven unknowns $A, B,\ p_B,\ p_D,\ \rho_B,\ \rho_D$ and β. To obtain a solution of the field equations, we assume that the shear scalar (σ) in these models is proportional to expansion scalar (θ).

This condition leads to,

$$A = B^n \tag{14}$$

Where A and B are the metric potentials and n is an arbitrary constant. Then, from the field equations, we get

$$A = c_1 t^{\frac{n}{3n-1}} \tag{15}$$

$$B = c_2 t^{\frac{1}{3n-1}} \tag{16}$$

Where c_1 and c_2 are constants.

Using equation (15) and (16) in equation (1), the line element can now be written as

$$ds^2 = dt^2 - c_1^2 t^{\frac{2n}{3n-1}}(dx^2 + dy^2 + dz^2) - c_2^2 t^{\frac{2}{3n-1}} d\psi^2 \tag{17}$$

The physical parameters of the model, like spatial volume (V), Hubble parameter (H), expansion scalar (θ), shear scalar (σ^2), anisotropic parameter (Δ) and deceleration parameter (q), are given by,

$$V = ct^{\frac{n}{3n-1}} \tag{18}$$

$$H = \frac{1}{4}\frac{3n+1}{3n-1}\frac{1}{t} \tag{19}$$

$$\theta = 4H = \frac{3n+1}{3n-1}\frac{1}{t} \tag{20}$$

$$\Delta = \frac{3(n-1)^2}{(3n-1)^2} \tag{21}$$

$$\sigma^2 = \frac{3}{8}\frac{(n-1)^2}{(3n-1)^2}\frac{1}{t^2} \tag{22}$$

$$q = \frac{9n-5}{3n+1} \tag{23}$$

$$\beta = \frac{1}{A^3B} = ct^{-\frac{3n+1}{3n-1}} \tag{24}$$

$$\lim_{t\to\infty}\frac{\sigma^2}{\theta^2} = \frac{3(n-1)^2}{8(3n+1)^2} \neq 0 \tag{26}$$

Graphs of physical parameters are drawn below.

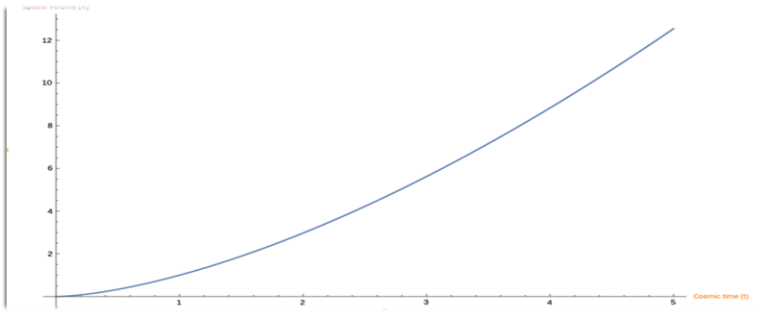

Fig. 1. Graph of spatial volume (V) versus time (t)

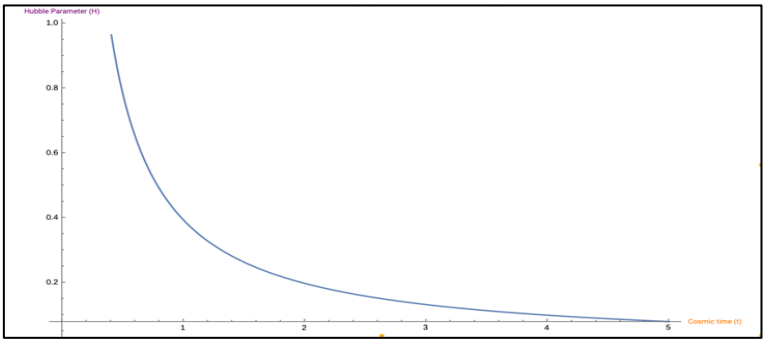

Fig. 2. Graph of Hubble parameter (H) versus time (t)

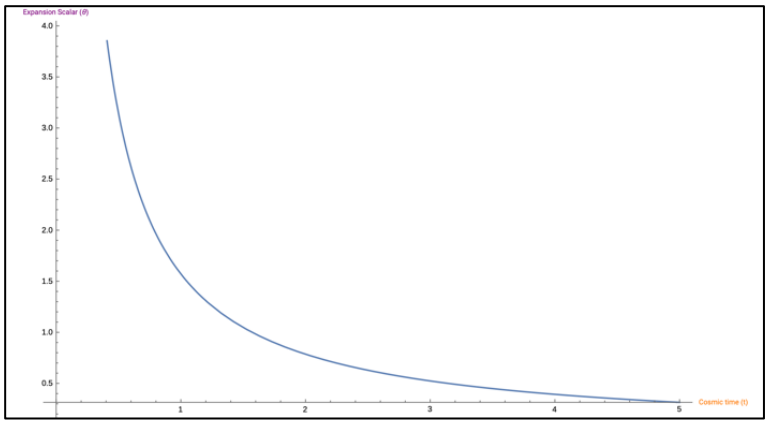

Fig. 3. Graph of expansion scalar (θ) versus cosmic time (t)

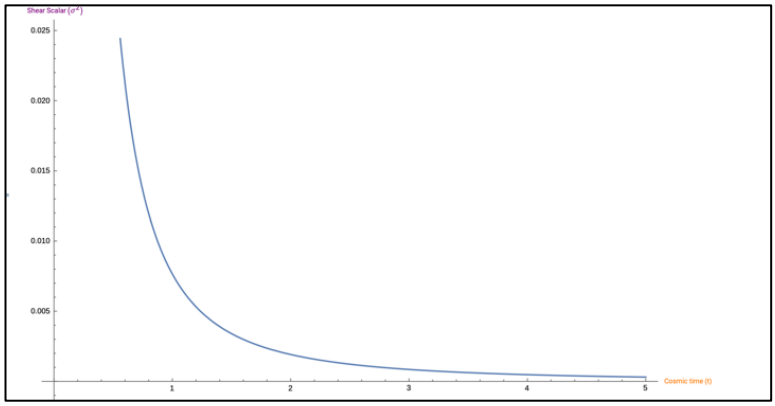

Fig. 4. Graph of shear scalar (σ^2) versus cosmic time (t)

It can be seen from Fig. 1 that the Spatial volume $V = 0$ $t = 0$ and it increases with time and tends to infinity as $t \to \infty$. Fig. 2 shows that the Hubble parameter (H) diverges for the initial time (t), and it decreases with increasing time and tends to zero as $t \to \infty$. From Fig. 3, the expansion scalar (θ) diverges for initial time (t) and decreases with time tending to zero as $t \to \infty$. From Fig. 4, the shear scalar (σ^2) diverges through initial time (t) and decreases over time, approaching zero as $t \to \infty$.

Further we consider two conditions of the fluids: a) Non-interacting two fluid model and b) Interacting two fluid model.

4.1 Non-interacting two fluid model

The conservation equation for the barotropic fluid and dark energy separately gives,

$$\dot{\rho_B} + 4H(p_B + \rho_B) = 0 \tag{26}$$

$$\dot{\rho_D} + 4H(p_D + \rho_D) = 0 \tag{27}$$

Integrating equation (26), we get

$$\rho_B = c_1 t^{-\frac{(\omega_B+1)(3n+1)}{(3n-1)}} \tag{28}$$

Substituting value of ρ_B from equation (28) in equation (10), we get

$$\rho_D = \frac{3n(n+1)}{(3n-1)^2 8\pi}\frac{1}{t^2} - ct^{-\frac{(\omega_B+1)(3n+1)}{(3n-1)}} + \frac{3}{32\pi}t^{-\frac{2(3n+1)}{(3n-1)}} \tag{29}$$

Substituting value of ρ_D in (27), we get

$$p_D = \frac{9n(n^2-1)}{8\pi(3n-1)^2(3n+1)}\frac{1}{t^2} - c\omega_B t^{-\frac{(\omega_B+1)(3n+1)}{(3n-1)}} + \frac{3}{32\pi}t^{-\frac{2(3n+1)}{(3n-1)}} \tag{30}$$

$$\omega_D = \frac{p_D}{\rho_D} = \frac{\frac{9n(n^2-1)}{8\pi(3n-1)^2(3n+1)}\frac{1}{t^2} - c\omega_B t^{-\frac{(\omega_B+1)(3n+1)}{(3n-1)}} + \frac{3}{32\pi}t^{-\frac{2(3n+1)}{(3n-1)}}}{\frac{3n(n+1)}{(3n-1)^2 8\pi}\frac{1}{t^2} - ct^{-\frac{(\omega_B+1)(3n+1)}{(3n-1)}} + \frac{3}{32\pi}t^{-\frac{2(3n+1)}{(3n-1)}}} \tag{31}$$

The expressions of Barotropic fluid density parameter (Ω_B) and Dark energy density parameter (Ω_D) are given by,

$$\Omega_B = \frac{\rho_B}{6H^2} = \frac{8c(3n-1)^2}{3(3n+1)^2}t^{2-\frac{(\omega_B+1)(3n+1)}{(3n-1)}} \tag{32}$$

$$\Omega_D = \frac{\rho_D}{6H^2} = \frac{n(n+1)}{(3n+1)^2} - \frac{8c(3n-1)^2}{3(3n+1)^2}t^{2-\frac{(\omega_B+1)(3n+1)}{(3n-1)}} + \frac{(3n-1)^2}{4\pi(3n+1)^2}t^{2-\frac{2(3n+1)}{(3n-1)}} \tag{33}$$

The total energy density (Ω) is given by,

$$\Omega = \Omega_B + \Omega_D = \frac{n(n+1)}{(3n+1)^2} + \frac{(3n-1)^2}{4\pi(3n+1)^2}t^{2-\frac{2(3n+1)}{(3n-1)}} \tag{34}$$

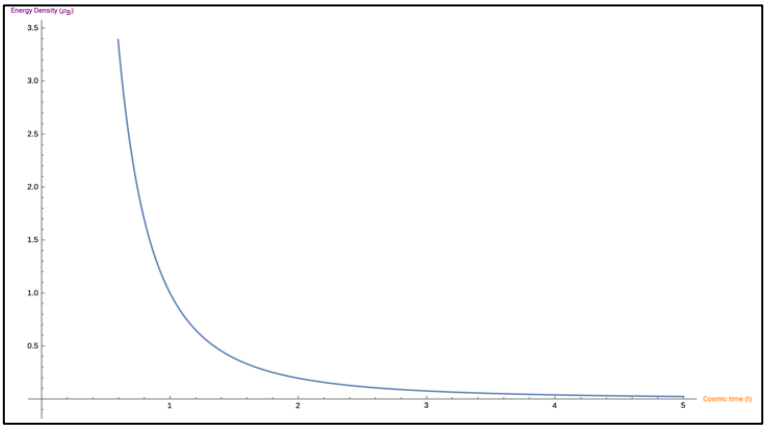

Fig. 5. Graph of ρ_B versus cosmic time (t) for non-interacting two fluid scenario.

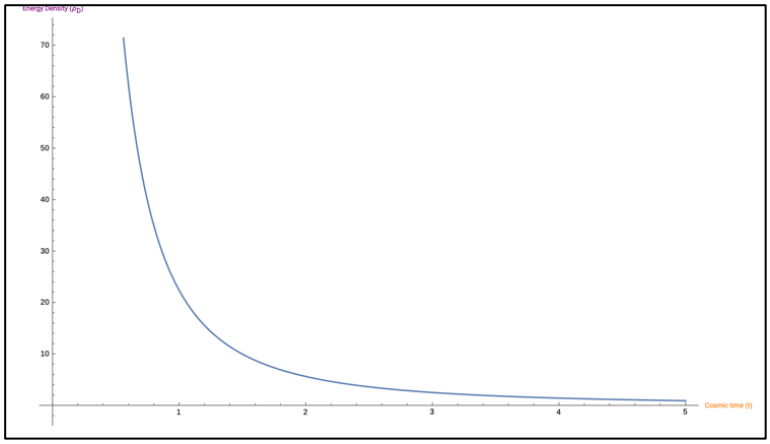

Fig. 6. Graph of ρ_D versus cosmic time (t) for non-interacting two fluid scenario.

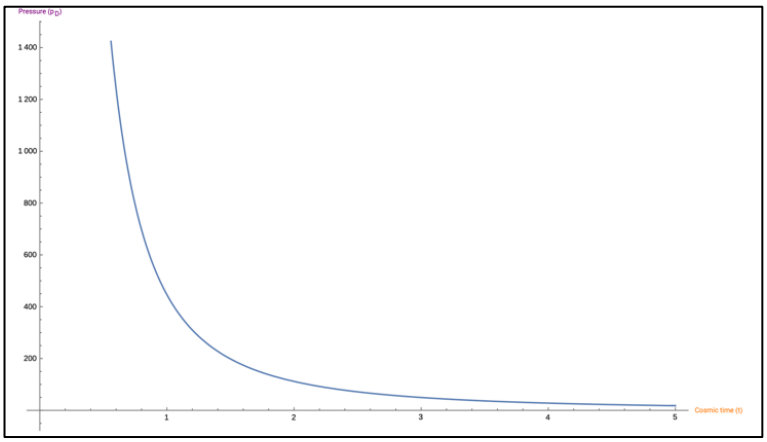

Fig. 7. Graph of p_D versus cosmic time (t) for non-interacting two fluid scenario.

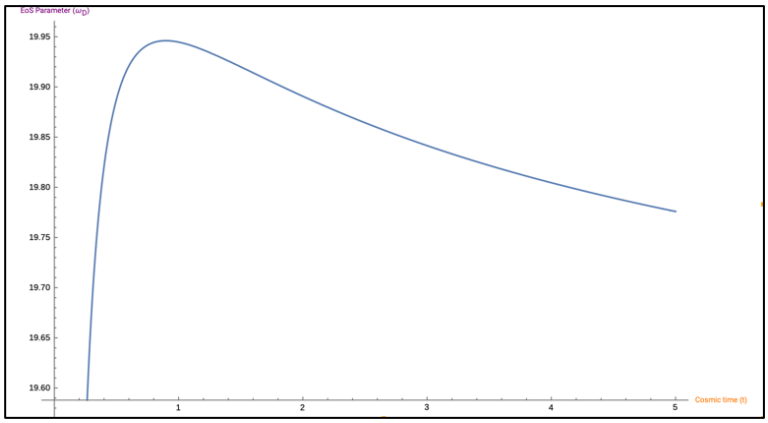

Fig. 8. Graph of ω_D versus cosmic time (t) for non-interacting two fluid scenario.

For non-interacting two fluid model, Fig. 5, shows the graph of ρ_B with cosmic time (t). It can be observed that ρ_B diverges at the initial instant (t) and decreases with time, and tends to zero as $t \to \infty$. Fig. 6 shows that the graph of ρ_D diverges at the initial time (t) and decreases with time, tending to zero as $t \to \infty$. Fig. 7, shows the Dark energy pressure (p_D) diverging at an initial time (t) and decreasing with time down to zero as $t \to \infty$. In Fig. 8, the Dark energy EoS parameter (ω_D) starts from the quintessence region $(\omega_D > -1)$ and remains in the quintessence region for the whole cosmic time (t).

4.2 Interacting two fluid model

In this section, we can write the energy conservation equation for the barotropic fluid and dark energy,

$$\dot{\rho_B} + 4H(p_B + \rho_B) = Q \tag{35}$$

$$\dot{\rho_D} + 4H(p_D + \rho_D) = -Q \tag{36}$$

We can write the above equation as,

$$\dot{\rho_B} + 4H(1 + \omega_B)\rho_B = Q \tag{37}$$

$$\dot{\rho_D} + 4H(1 + \omega_D)\rho_D = -Q \tag{38}$$

Where $\omega = \frac{p}{\rho}$ and the quantity Q represents the interaction between Barotropic fluid and Dark energy components. We consider $Q > 0$, this ensures that the energy being transferred from Dark energy to Barotropic fluid.

Consider, $Q = 4Hk\rho_B$, where k is a coupling constant,

Using above value of Q in equation (37), we get

$$\rho_B = ct^{(k-\omega_B-1)\frac{(3n+1)}{(3n-1)}} \tag{39}$$

$$\rho_D = \frac{3n(n+1)}{8\pi(3n-1)^2}\frac{1}{t^2} - ct^{(k-\omega_B-1)\frac{(3n+1)}{(3n-1)}} - \frac{3}{32\pi}t^{-\frac{2(3n+1)}{(3n-1)}} \tag{40}$$

Substituting the value of ρ_D in equation (36), we get

$$p_D = \frac{9n(n-1)^2}{8\pi(3n-1)^2(3n+1)}\frac{1}{t^2} + c(1-\omega_B)t^{(k-\omega_B-1)\frac{(3n+1)}{(3n-1)}} - \frac{3}{32\pi}t^{-\frac{2(3n+1)}{(3n-1)}} \tag{41}$$

$$\omega_D = \frac{p_D}{\rho_D} = \frac{\frac{9n(n-1)^2}{8\pi(3n-1)^2(3n+1)}\frac{1}{t^2} + c(1-\omega_B)t^{(k-\omega_B-1)\frac{(3n+1)}{(3n-1)}} - \frac{3}{32\pi}t^{-\frac{2(3n+1)}{(3n-1)}}}{\frac{3n(n+1)}{8\pi(3n-1)^2}\frac{1}{t^2} - ct^{(k-\omega_B-1)\frac{(3n+1)}{(3n-1)}} - \frac{3}{32\pi}t^{-\frac{2(3n+1)}{(3n-1)}}} \tag{42}$$

The expressions of Barotropic fluid density parameter (Ω_B) and Dark energy density parameter (Ω_D) are given as,

$$\Omega_B = \frac{\rho_B}{6H^2} = \frac{8c(3n-1)^2}{3(3n+1)^2}t^{2+\frac{(k-\omega_B-1)(3n+1)}{(3n-1)}} \tag{43}$$

$$\Omega_D = \frac{\rho_D}{6H^2} = \frac{n(n+1)}{\pi(3n+1)^2} - \frac{8c(3n-1)^2}{3(3n+1)^2}t^{2+\frac{(k-\omega_B-1)(3n+1)}{3n-1}} - \frac{(3n-1)^2}{4\pi(3n+1)^2}t^{2-\frac{2(3n+1)}{(3n-1)}} \tag{44}$$

The total energy density (Ω) is given by,

$$\Omega = \Omega_B + \Omega_D = \frac{n(n+1)}{\pi(3n+1)^2} - \frac{(3n-1)^2}{4\pi(3n+1)^2}t^{2-\frac{2(3n+1)}{(3n-1)}} \tag{45}$$

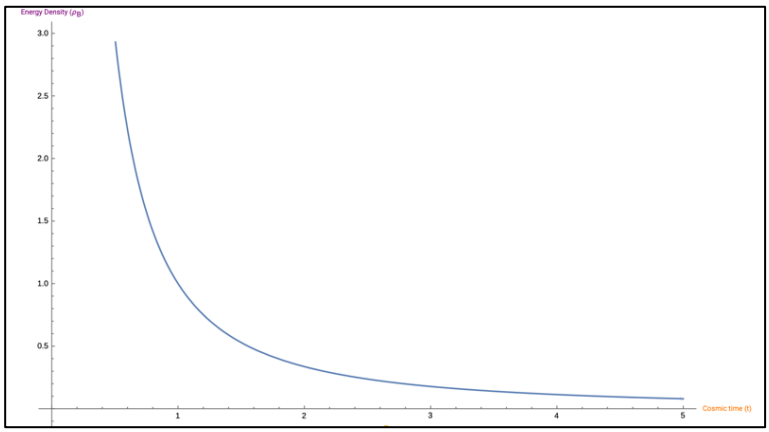

Fig. 9. Graph of ρ_B versus cosmic time (t) for interacting two fluid scenario.

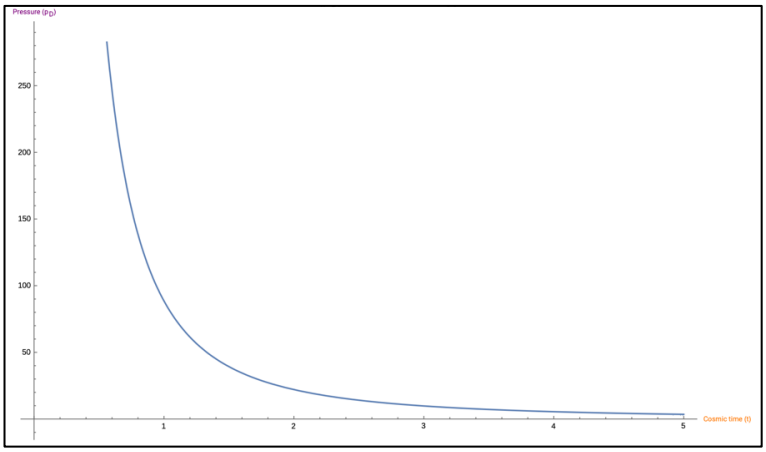

Fig. 10. Graph of p_D versus cosmic time (t) for interacting two fluid scenario.

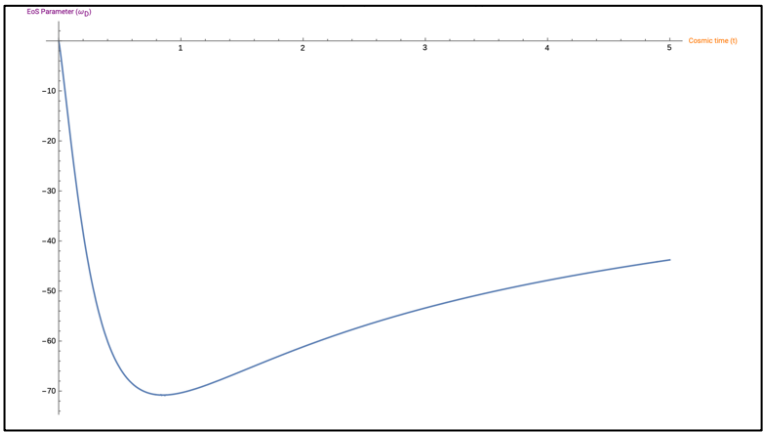

Fig. 11. Graph of ω_D versus cosmic time (t) for interacting two fluid scenario.

For interacting two fluid model, Fig. 9, shows the graph of ρ_B with cosmic time (t). It is observed that ρ_B diverges for initial time (t) and it decreases with time and tends to zero as $t \to \infty$. Figure 10, shows the graph of p_D with cosmic time (t). It is observed from the graph that p_D diverges for $t = 0$ and tends to zero as $t \to \infty$. Figure 11, represents the graph of EoS parameter of Dark energy (ω_D) with cosmic time (t). It shows that $\omega_D = 0$ when $t = 0$ i.e., initially ω_D is in quintessence region and as $t \longrightarrow \infty$, ω_D crosses PDE $(\omega_D = -1)$ and finally stables in phantom region $(\omega_D < -1)$.

5. Cosmological Parameters:

5.1 Look Back time: The look back time t_L is given by,

$$t_L = t_0 - t(z) = \int_R^{R_0} \frac{dR}{R} \tag{46}$$

The relation between scale factor t_L and redshift parameter (z) is given below,

$$\frac{R}{R_0} = \frac{1}{1+z} \tag{47}$$

Using equation (47) in equation (46), we get

$$t_L = \frac{3n+1}{H_0 4(3n-1)}\left[1-(1+z)^{-\frac{4(3n-1)}{(3n+1)}}\right] \tag{48}$$

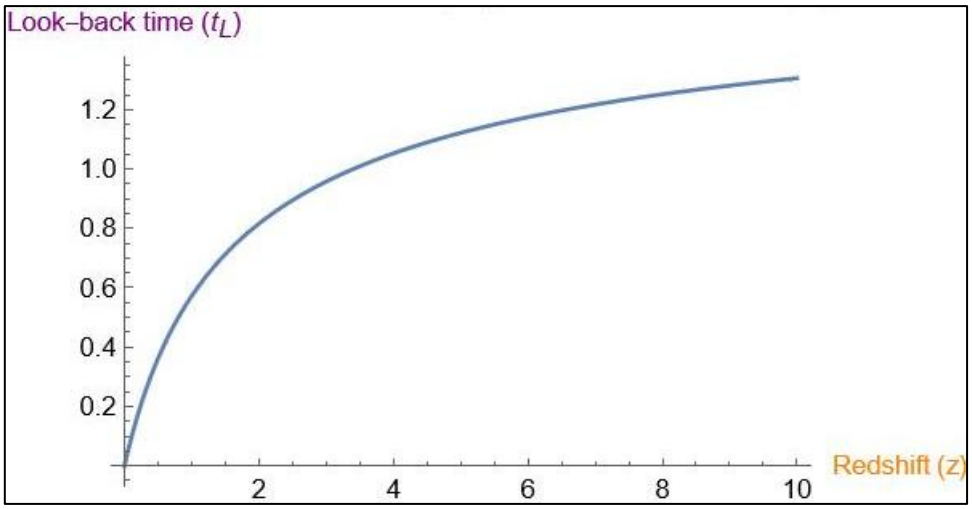

Fig. 12. Graph of t_L versus Redshift (z)

5.2 Proper Distance: The proper distance $d(z)$ is given by,

$$d(z) = r_1 R_0 \tag{49}$$

Where, $r_1 = \int_t^{t_0} \frac{dt}{R}$ (50)

From equation (49) and (50), we get

$$d(z) = \frac{R_0 k'}{k\left[1 - \frac{3n+1}{4(3n-1)}\right]}\left[1 - (1+z)^{1-\frac{4(3n-1)}{(3n+1)}}\right] \tag{51}$$

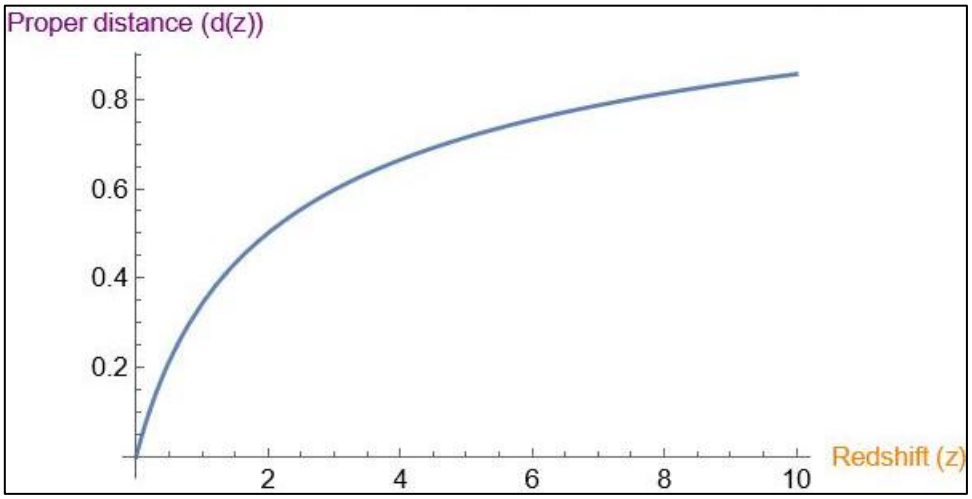

Fig. 13. Graph of $d(z)$ versus Redshift (z)

5.3 Luminosity Distance: Luminosity distance (d_L) is given by,

$$d_L = r_1(z) R_0 (1+z) = d(z)(1+z) \tag{52}$$

Substituting value of $d(z)$ from equation (51) in equation (52), we get

$$d_L = \frac{R_0 k'}{k\left[1 - \frac{3n+1}{4(3n-1)}\right]}\left[1 - (1+z)^{1-\frac{4(3n-1)}{(3n+1)}}\right](1+z) \tag{53}$$

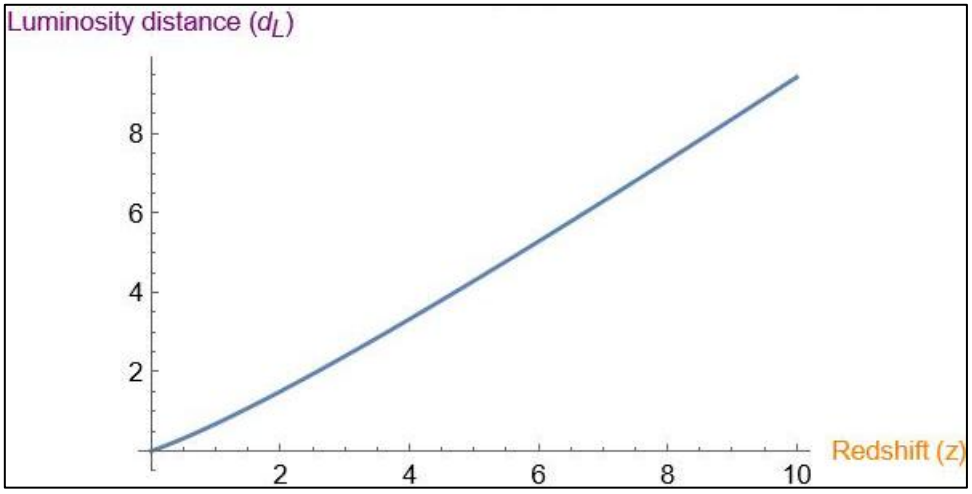

Fig. 14. Graph of d_L versus Redshift (z)

5.4 Angular Diameter Distance: Angular diameter distance d_A is given by,

$$d_A = d(z)(1+z)^{-1} \tag{54}$$

Substituting value of $d(z)$ from equation (51) in equation (54), we get

$$d_A = \frac{R_0 k'}{k\left[1-\frac{3n+1}{4(3n-1)}\right]}\left[1-(1+z)^{1-\frac{4(3n-1)}{(3n+1)}}\right](1+z)^{-1} \tag{55}$$

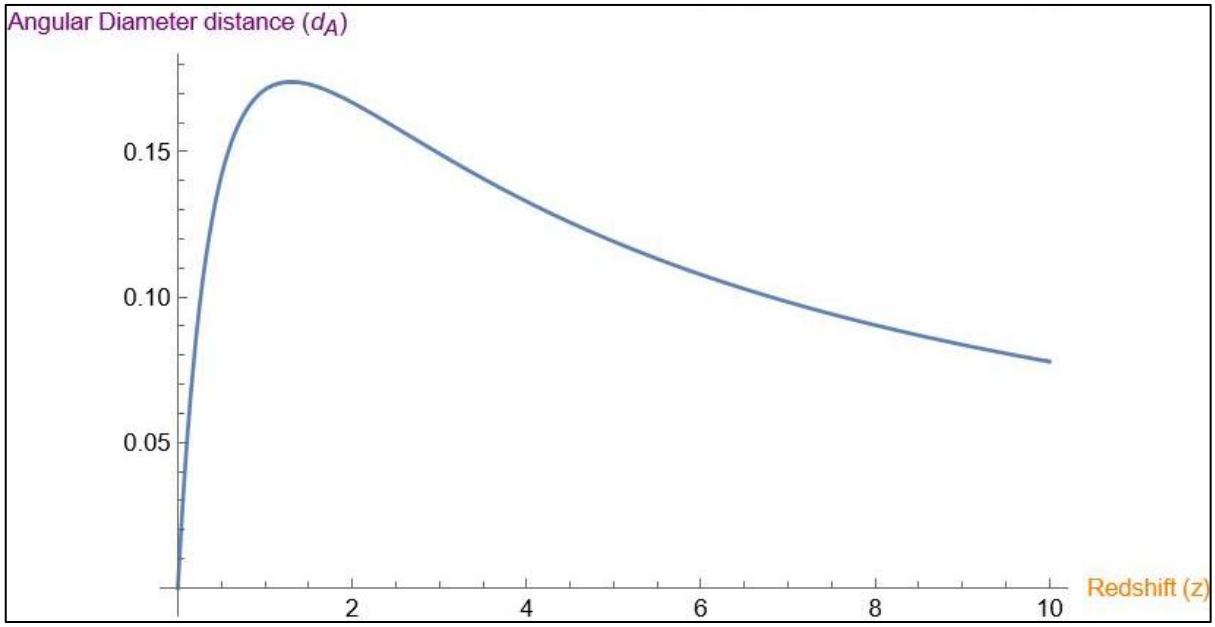

Fig. 15. Graph of d_A versus Redshift (z)

5.5 Distance Modulus: The distance modulus $\mu(z)$ is given by

$$\mu(z) = 5\log d_L + 25 \tag{56}$$

Substituting value of d_L from equation (53) in equation (56), we get

$$\mu(z) = 5\log\frac{R_0 k'}{k\left[1-\frac{3n+1}{4(3n-1)}\right]}\left[1-(1+z)^{1-\frac{4(3n-1)}{(3n+1)}}\right](1+z)+25 \qquad (57)$$

6. Conclusion

In the present paper, we have studied a five-dimensional Kaluza-Klein cosmological model filled with barotropic fluid and dark energy in Lyra geometry by considering the shear scalar (σ) proportional to the expansion scalar(θ). We have derived physical and kinematical parameters for both the interacting and non-interacting scenarios. In the physical parameters, spatial volume (V) increases with cosmic time(t), resulting in a model that begins to evolve at an initial instant with zero volume and an infinite expansion rate. The Hubble parameter(H), expansion scalar (θ) and the shear scalar (σ^2) diverges for initial time(t), and it decreases as time increases and tends to zero as $t \to \infty$. At the same time, the displacement vector (β) decreases and tends to zero as $t \to \infty$. The recent observations of Supernovae-Ia reveal that the present universe is accelerating, and the value of the deceleration parameter (q) lie somewhere in the range $-1 \leq q \leq 0$. Since $q < 0$ for $\frac{1}{3} < n \leq \frac{5}{9}$, the inclusion of the dark energy into the system gives rise to an accelerated expansion of the universe. Equation (25) and (21) shows that $\lim_{t\to\infty}\frac{\sigma^2}{\theta^2} \neq 0$, and the anisotropic parameter (Δ) does not vanish for $\frac{1}{3} < n \leq \frac{5}{9}$. Hence, this model does not tend to isotropy. Hence, our model is totally anisotropic and spatially homogeneous. For both interacting and non-interacting cases, the pressure and density of Dark energy and Barotropic fluid diverge for initial cosmic time (t) and tends to zero as $t \to \infty$. We also consider the consistency of our models with observational parameters such as look-back time, proper distance, luminosity distance, angular diameter and distance modulus. The solutions obtained are consistent with recent observational results.

Acknowledgement

One of the authors P. W. Gaidhane is grateful to the University Grants Commission (UGC) New Delhi, for providing the financial assistance.

6. Reference

1. Perlmutter S, Gabi S, Goldhaber G, Goobar A, Groom DE, Hook IM, Kim AG, Kim MY, Lee JC, Pain R, Pennypacker CR. Measurements* of the Cosmological Parameters Ω and Λ from the First Seven Supernovae at z≥ 0.35. The astrophysical journal. 1997 Jul 10;483(2):565. Doi: 10.1086/304265

2. Perlmutter S, Aldering G, Valle MD, Deustua S, Ellis RS, Fabbro S, Fruchter A, Goldhaber G, Groom DE, Hook IM, Kim AG. Discovery of a supernova explosion at half the age of the Universe. Nature. 1998 Jan 1;391(6662):51-4. https://doi.org/10.1038/34124

3. Perlmutter S, Aldering G, Goldhaber G, Knop RA, Nugent P, Castro PG, Deustua S, Fabbro S, Goobar A, Groom DE, Hook IM. Measurements of Ω and Λ from 42 high-redshift supernovae. The Astrophysical Journal. 1999 Jun 1;517(2):565. Doi: 10.1086/307221

4. Riess AG, Filippenko AV, Challis P, Clocchiatti A, Diercks A, Garnavich PM, Gilliland RL, Hogan CJ, Jha S, Kirshner RP, Leibundgut BR. Observational evidence from supernovae for an accelerating universe and a cosmological constant. The astronomical journal. 1998 Sep 1;116(3):1009. Doi: 10.1086/300499

5. Weinberg S. The cosmological constant problem. Reviews of modern physics. 1989 Jan 1;61(1):1.

https://doi.org/10.1103/RevModPhys.61.1

6. Peebles PJ, Vilenkin A. Quintessential inflation. Physical Review D. 1999 Feb 12;59(6):063505.

https://doi.org/10.1103/PhysRevD.59.063505

7. Akarsu Ö, Kılınç CB. LRS Bianchi type I models with anisotropic dark energy and constant deceleration parameter. General Relativity and Gravitation. 2010 Jan;42:119-40. https://doi.org/10.1007/s10714-009-0821-y

8. Akarsu Ö, Kılınç CB. Bianchi type III models with anisotropic dark energy. General Relativity and Gravitation. 2010 Apr;42(4):763-75. https://doi.org/10.1007/s10714-009-0878-7

9. Yadav AK, Rahaman F, Ray S. Dark energy models with variable equation of state parameter. International Journal of Theoretical Physics. 2011 Mar;50:871-81. https://doi.org/10.1007/s10773-010-0628-3

10. Yadav AK, Yadav L. Bianchi type III anisotropic dark energy models with constant deceleration parameter. International Journal of Theoretical Physics. 2011 Jan;50:218-27. https://doi.org/10.1007/s10773-010-0510-3

11. Kumar S, Akarsu Ö. Bianchi type-II models in the presence of perfect fluid and anisotropic dark energy. The European Physical Journal Plus. 2012 Jun;127:1-3. https://doi.org/10.1140/epjp/i2012-12064-4

12. Amendola L. Coupled quintessence. Physical Review D. 2000 Jul 24;62(4):043511. https://doi.org/10.1103/PhysRevD.62.043511

13. Szydłowski M, Kurek A, Krawiec A. Top ten accelerating cosmological models. Physics Letters B. 2006 Nov 9;642(3):171-8. https://doi.org/10.1016/j.physletb.2006.09.052

14. Setare MR. Interacting holographic dark energy model and generalized second law of thermodynamicsin a non-flat universe. Journal of Cosmology and Astroparticle Physics. 2007 Jan 24;2007(01):023. 10.1088/1475-7516/2007/01/023

15. Pradhan A, Amirhashchi H, Saha B. An interacting and non-interacting two-fluid scenario for dark energy in FRW universe with constant deceleration parameter. Astrophysics and Space Science. 2011 May;333:343-50. https://doi.org/10.1007/s10509-011-0626-9

16. Amirhashchi H, Pradhan A, Saha B. An Interacting Two-Fluid Scenario for Dark Energy in an FRW Universe. Chinese Physics Letters, 28(3), 039801 (2011). https://doi.org/10.1088/0256-307x/28/3/039801

17. Amirhashchi H, Pradhan A, Zainuddin H. An interacting and non-interacting two-fluid dark energy models in FRW universe with time dependent deceleration parameter. International Journal of Theoretical Physics. 2011 Nov;50:3529-43. https://doi.org/10.1007/s10773-011-0861-4

18. Saha B, Amirhashchi H, Pradhan A. Two-fluid scenario for dark energy models in an FRW universe-revisited. Astrophysics and Space Science. 2012 Nov;342(1):257-67. https://doi.org/10.1007/s10509-012-1155-x

19. Weyl H. Gravitation and Electricity. *Sitzungsber.Preuss.Akad.Wiss.Berlin (Math.Phys.)* 1918 (1918) 465

20. Sen DK. A Static Cosmological Model. Zeitschrift für Physik A Hadrons and Nuclei, Vol. 149, No. 3, 1957, pp. 311-323. https://doi.org/10.1007/bf01333146

21. Sen DK and Dunn KA. A Scalar-Tensor Theory of Gravitation in a Modified Riemannian Manifold. Journal of Mathematical Physics, Vol. 12, No. 4, 1971, pp. 578-586. doi:10.1063/1.1665623

22. Halford WD. SCALAR--TENSOR THEORY OF GRAVITATION IN A LYRA MANIFOLD. Massey Univ., Palmerston North, New Zealand; 1972 Jan 1. https://doi.org/10.1063/1.1665894

23. Mete VG, Deshmukh V. Five-Dimensional Cosmological Model with One Dimensional Cosmic String Coupled with Zero Mass Scalar Field in Lyra Manifold. Journal of Scientific Research. 2023 May 1;15(2):351-9. https://doi.org/10.3329/jsr.v15i2.61442

24. Lambat PM, Pund AM. Bianchi Type-VI0 Inflationary Model in Lyra Geometry. Journal of Scientific Research. 2022 May 6;14(2):435-42. https://doi.org/10.3329/jsr.v14i2.55557

25. Aditya Y, Divya Prasanthi UY, Reddy DR. Bianchi type-IX model in the presence of anisotropic dark energy and massive scalar meson field in Lyra geometry. International Journal of Modern Physics A. 2022 Jun 10;37(16):2250107. https://doi.org/10.1142/s0217751x2250107x

26. Singh JK, Singh P, Saridakis EN, Myrzakul S, Balhara H. New parametrization of the dark-energy equation of state with a single parameter. Universe. 2024 Jun 1;10(6):246. https://doi.org/10.1142/s0218271823500402

27. Bishi BK, Lepse PV. Particle creation and quadratic deceleration parameter in Lyra geometry. New Astronomy. 2021 May 1;85:101563. https://doi.org/10.1016/j.newast.2020.101563

28. Witten E. Some properties of O (32) superstrings. Physics Letters B. 1984 Dec 20;149(4-5):351-6. https://doi.org/10.1016/0370-2693(84)90422-2

29. Appelquist T, Chodos A, Freund PG. Modern Kaluza-Klein Theories. (No Title). 1987.

30. Kaluza T. Sitzungsber. Preuss. Akad. Wiss. Phys. Math. Klasse. 1921.

31. Klein O. Quantentheorie und fünfdimensionale Relativitätstheorie. Zeitschrift für Physik. 1926 Dec;37(12):895-906. https://doi.org/10.1007/BF01397481

32. Chodos A, Detweiler S. Where has the fifth dimension gone?. Physical Review D. 1980 Apr 15;21(8):2167. https://doi.org/10.1103/physrevd.21.2167

33. Freund PGO, Hawking S. The Pontifical Academy of Sciences.

34. Pawar DD, Jakore BL, Dagwal VJ. Kaluza–Klein cosmological model with strange-quark-matter in Lyra geometry. International Journal of Geometric Methods in Modern Physics. 2023 Apr 31;20(05):2350079. https://doi.org/10.1142/s0219887823500792

35. Aditya Y, Raju KD, Rao VU, Reddy DR. Kaluza-Klein dark energy model in Lyra manifold in the presence of massive scalar field. Astrophysics and Space Science, 364(11) (2019). https://doi.org/10.1007/s10509-019-3681-2

36. Mishra AK, Sharma UK, Pradhan A. A comparative study of Kaluza–Klein model with magnetic field in Lyra manifold and general relativity. New Astronomy. 2019 Jul1;70:27-35. https://doi.org/10.1016/j.newast.2019.02.003

37. Mete VG, Bansod AS, Murade PB. Accelerating Anisotropic Bianchi Type-V Model with Barotropic Matter and Viscous Dark Energy in Lyra Geometry. International Journal of Mathematics Trends and Technology-IJMTT. 2020;66.

doi:10.14445/22315373/IJMTT-V66I11P510.

38. Trivedi D, Bhabor AK. Higher-dimensional Bianchi type-I dark energy models with barotropic fluid in Saez-Ballester scalar-tensor theory of gravitation. Indian Journal of Physics. 2023 Apr;97(4):1317-27. https://doi.org/10.1007/s12648-022-02448-3

39. Vijaya Santhi M, Rao VU, Aditya Y. Kaluza-klein cosmological models with two fluids source in brans-dicke theory of gravitation. The African Review of Physics. 2016 Dec 13;11.